Scarring by short pieces of bifurcated periodic orbits

epl A Letters Journal Exploring the Frontiers of Physics

March 2011

EPL, **93** (2011) 60005
doi: 10.1209/0295-5075/93/60005

www.epljournal.org

Scarring by short pieces of bifurcated periodic orbits

A. A. Zembekov[1,2], R. M. Benito[1] and F. Borondo[3(a)]

[1] *Grupo de Sistemas Complejos and Departamento de Física, Escuela Técnica Superior de Ingenieros Agrónomos, Universidad Politécnica de Madrid - 28040 Madrid, Spain, EU*
[2] *Institute of Chemical Physics, Russian Academy of Sciences - Moscow, Russia*[(b)]
[3] *Departamento de Química, and Instituto Mixto de Ciencias Matemáticas CSIC-UAM-UC3M-UCM, Universidad Autónoma de Madrid - Cantoblanco, 28049 Madrid, Spain, EU*

received 24 January 2011; accepted in final form 24 February 2011
published online 24 March 2011

PACS 05.45.Mt – Quantum chaos; semiclassical methods
PACS 03.65.Sq – Semiclassical theories and applications

Abstract – A non-conventional mechanism for scarring in generic Hamiltonian systems with mixed dynamics, taking place through the combined focusing and defocusing effect of focal points of short pieces of bifurcated orbits, is discussed.

Introduction. – Scar theory [1,2] has been a subject of much interest since the publication of Heller's seminal paper [3]. It describes an enhanced localization of quantum probability density along short unstable periodic orbits (POs) that appears in certain individual eigenfunctions of classically chaotic systems, this being important since it implies a dramatic departure from the predictions of random matrix theory [4]. Scarred structures were systematically studied by Heller [3], who constructed a theory based on wave packet propagation [5]. Another key contribution to the theory of scars is due to Bogomolny [6], who derived an explicit expression for the smoothed probability density over small ranges of space and energy. *i.e.* averaged over a large number of eigenfunctions semiclassically [7,8]. A corresponding theory for Wigner functions was developed by Berry [9]. Scars have also been observed experimentally [10–13].

The situation is, however, quite different in the case of generic systems with mixed (regular and chaotic) dynamics where scarring has been much less studied. Some results [14,15] should, nevertheless, be mentioned. Special consideration deserves the work of Keating and Prado [14] who showed, by considering scaling laws in an extension of Bogomolny's theory, that scars of quantum eigenfunctions by classical PO may be dramatically enhanced when these orbits undergo bifurcations. This "superscarring" manifests as a stronger localization on wider regions of configuration space than in the case of the scars corresponding to isolated POs.

In this letter, we discuss an unconventional mechanism of scarring that happens in systems with mixed dynamics due to the effect of short pieces of (long) bifurcated orbits. We show how the building-up of quantum (and classical) density takes place as the result of the interplay between focusing and defocusing caused by neighboring focal points (FPs) in the orbits of an infinite series of period-doubling saddle-node bifurcations (SNB). This mechanism "dresses" a particular area of configuration space by pieces of different orbits, which arise in the Farey tree of the original PO, or even by pieces of orbits which have nothing to do with the central bifurcated PO. As an illustration, we discuss this effect in a realistic model for the vibrations of the LiNC/LiCN triatomic molecule, where it can greatly affect many aspects of the associated dynamics, such as for example the isomerization process LiNC $\rightleftharpoons$ LiCN.

System. – The vibrational dynamics of the LiNC/LiCN isomerizing molecular system has been extensively studied in the past in connection with the issue of quantum chaos [16,17]. For example, in ref. [18] the superscarring effect of a pair of 1 : 1 SNB POs [19] was considered.

This system can be modelled by the 2-dof Hamiltonian

$$H = \frac{P_R^2}{2\mu_1} + \frac{1}{2}\left(\frac{1}{\mu_1 R^2} + \frac{1}{\mu_2 r_e^2}\right) P_\vartheta^2 + V(R,\vartheta), \qquad (1)$$

where R and ϑ are Jacobi coordinates specifying the position of the Li atom with respect to the center of mass of the CN fragment. The C-N distance is kept frozen at its equilibrium value, r_e, since this motion is of sufficiently

(a) E-mail: f.borondo@uam.es
(b) Permanent address.

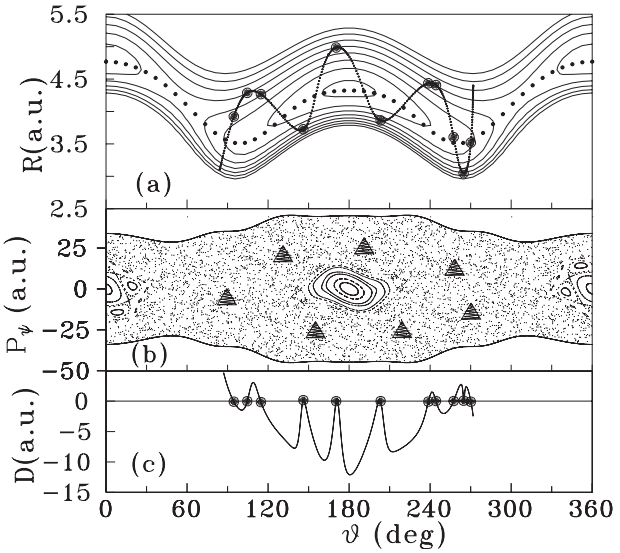

Fig. 1: (a) Potential energy surface for LiNC/LiCN. The minimum energy path (dotted line), a 1 : 7 asymmetrical periodic orbit (full line) relevant to our work, and its focal points (full circles) are also plotted. (b) Composite Poincaré surface of section at $E = 5080.51\,\mathrm{cm}^{-1}$. The fixed points of the 1 : 7 periodic orbit are indicated by full triangles. (c) Function D in the pre-exponential factor of eq. (3) calculated along the 1 : 7 periodic orbit. Zeroes correspond to focal points.

high frequency to effectively decouple from the rest of vibrational coordinates of the molecule. The interaction potential is shown in fig. 1(a) as a contours plot. It presents two wells, at $\vartheta = 0$ and 180°, corresponding to the linear isomers LiCN and LiNC, which are separated by a modest energy barrier. The motion in ϑ is very floppy, and chaos sets in at very moderate values of the excitation vibrational energy.

Superimposed on the potential surface, we also present in fig. 1(a) a PO which is very relevant to our work. It corresponds to an asymmetrical 1 : 7 resonance embedded in the chaotic sea, which appears "out of the blue" in a SNB at $E = 4243.76\,\mathrm{cm}^{-1}$, due to a sudden variation of the adiabatic stretching frequency, and has a profound influence in the quantum mechanics of the system, both above and below ("ghost orbits") this energy [19]. The trajectory has two interesting "end-legs". The left one (as drawn in the figure), centered at $\vartheta \sim 110°$, is horseshoe shaped, and the one at the right end is a very narrow U, running almost vertical at $\vartheta \sim 265°$. The companion PO, born at the same SNB, is a close-lying 1 : 7 resonant trajectory with very similar topology, which is indistinguishable on the scale of the figure.

Classical dynamics. – The classical vibrational dynamics of our system, LiNC/LiCN, can be adequately followed by considering Poincaré surfaces of section (SOS), computed in our case by using the minimum energy path, $R_e(\vartheta)$, connecting the two isomers as the sectioning plane (see the dotted line in fig. 1(a)). This choice requires an additional canonical transformation,

$$\begin{aligned} \rho &= R - R_e(\vartheta), \quad & P_\rho &= P_R, \\ \psi &= \vartheta, & P_\psi &= P_\vartheta - \left(\frac{\mathrm{d}R_e}{\mathrm{d}\vartheta}\right)_{\vartheta=\psi} P_\rho, \end{aligned} \tag{2}$$

to make the SOS an area-preserving map (see ref. [20] for details). In fig. 1(b) we present a composite SOS for $E = 5080.51\,\mathrm{cm}^{-1}$, showing that the dynamics are mostly chaotic, with two islands of regularity corresponding to the two isomer wells.

Computational method. – Central to the spirit of this letter is the idea that scarring involves (in general) groups of neighboring eigenstates, the smoothing of which renders the localized structures [5–7]. Also, it is crucial the fact that in systems with mixed dynamics scarring appears most often only partially, due to other competing effects such as, for example, the high localization taking place in the existing regular regions, or the effect that we are presenting in this letter.

Taking this into account, we present in the top row of fig. 2 the wave functions, $|n\rangle$, of some representative states in one such group, centered around the energy considered in this work. They have been calculated using the discrete variable representation method, as implemented by Bacic and Light [21]. As can be seen, they all exhibit a noticeable scar from the horseshoe leg of the 1 : 7 PO of fig. 1(a). This localization is more easily seen in phase space and then we present in the bottom row of the figure the quantum SOS (QSOS) computed from the corresponding Husimi functions. To visually foster this effect, only the highest contours (> 50% of the maximum value) have been plotted. However, and as noted above, the scarring of the PO is only partial, in the sense that non-negligible probability density also exists around the wells where regular motion takes place.

To explain this unconventional scarring mechanism we use the semiclassical Green's function [22]

$$\begin{aligned} G(x,x';E) \;=\; & \frac{1}{\mathrm{i}\hbar} \sum_{\mathrm{traj}} \left|\frac{1}{vv'D}\right|^{1/2} \\ & \times \exp\left[\frac{\mathrm{i}}{\hbar} S(x,x';E) - \frac{\mathrm{i}\pi}{2}\nu\right], \end{aligned} \tag{3}$$

where the sum is taken over all trajectories connecting points x and x' at energy E, $S(x,x';E)$ is the classical action function, ν the Maslov index, and v and v' the velocity components along the orbit, respectively. From eq. (3), information on the wave functions of the system can be extracted by means of the quantum-mechanical expression

$$G(x,x';E) = \left\langle x \left| \frac{1}{E-\hat{H}} \right| x' \right\rangle = \sum_n \frac{\langle x|n\rangle\langle n|x'\rangle}{E-E_n}. \tag{4}$$

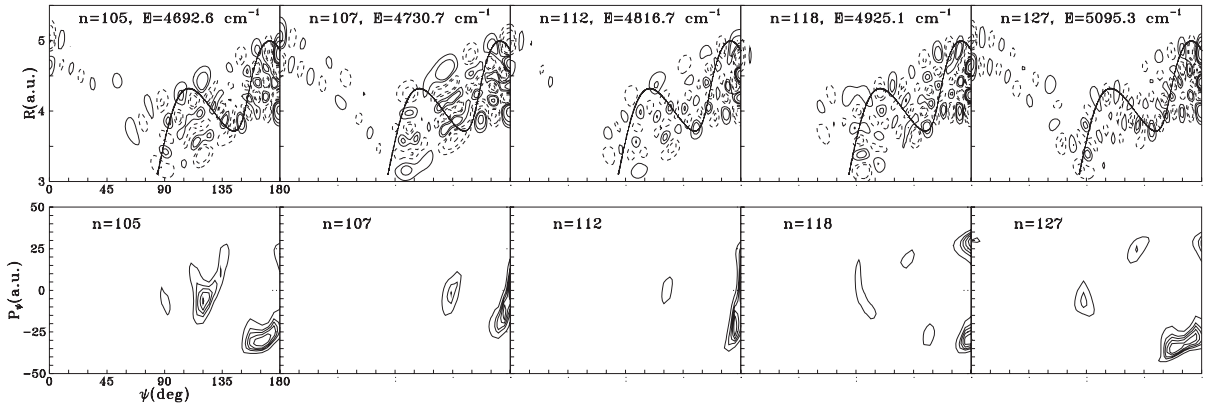

Fig. 2: Some LiNC/LiCN wave functions (top row) and the corresponding Husimi-based QSOS (bottom row) scarred by the horseshoe left-end of the 1 : 7 periodic orbit in fig. 1. Negative values of the wave functions are indicated by dashed lines.

Regularization by taking an average over a narrow energy window around the poles with $x = x'$ renders the following approximate expression for the quasi-wave functions [6]

$$\langle |\psi_n(x)|^2 \rangle \simeq \langle \mathrm{Im}\ G(x, x; E) \rangle. \tag{5}$$

It is important to notice that the contributions to the summation in (3) appear as products of two factors, with opposite effects. The first one is the amplitude or pre-exponential factor, that can produce a dramatic accumulation of density at the caustics, resulting in catastrophes [23]. It is determined by the classical density, $|vv'D|^{-1/2}$, whose matrix elements can be calculated quite efficiently using local coordinates [24], being related to the rate of divergence of trajectories starting at the same point with momenta pointing toward slightly different directions, and then with the "focusing" properties of the system dynamics. The second factor in the sum of (3) is a harmonic term that gives rise to complicated interferences, this tending to eliminate the previous accumulation patterns. Let us discuss next the effects of these two different terms in the problem addressed in this letter.

An unconventional scarring mechanism. – Superimposed on the 1 : 7 PO, we indicate in fig. 1(a) with full circles the position of the corresponding FPs, which correspond to the zeroes of the D-function (see fig. 1(c)). Aside from the five "normal" FPs, which are associated with turning points, and the two terminal ones, not appearing since v has been explicitly included in eq. (3), there are in this plot five additional FPs at intermediate positions. This is typical of bifurcated POs, due to the complexity inherent to the evolution process followed from their inception at the bifurcation to higher values of the energy [24]. In particular, most interesting for our purposes are the three leftmost FPs, located in the range $\vartheta = 90°$–$120°$, since it is in this region where the horseshoe leg of the PO scars the wave functions shown in fig. 2. Indeed, the behavior of D in this interval is quite notorious. Instead of crossing the horizontal axis, giving rise to simple zeroes that would correspond isolated FPs, the function develops a fold [23], originating three close lying zeroes and the same number of close lying FPs. Again, it should be remarked that this behavior is typical from bifurcated POs. Accordingly, the stability of the bifurcated orbit is not uniform along all its length, some pieces being more stable (smaller values of the local Lyapunov exponents) than others. The important point here is that greater stabilities imply larger values of the classical density. Therefore, it is feasible that short segments of long bifurcated orbits give rise to big localization effects, this being the hallmark of scars. In our case, it is evident from fig. 2 that only the first (and last) segments (or oscillations) of the PO produce scars, while the contribution from the middle part is much smaller. In this sense, it can be stated as a rule, that any bifurcated PO consists of "bright" and "dark" segments, contributing, respectively, to the scarred and (chaotic) background parts of the system eigenfunctions.

Let us consider now in more detail how this idea can be used as the basis to render a plausible mechanism explaining the existence of the horseshoe scars observed in the LiNC/LiCN eigenstates of fig. 2, or in general of partial scars in regions where no short POs with an adequate topology and symmetry exist. For this purpose, we show in fig. 3(a) the time evolution of a bunch of trajectories starting at point i, next to the leftmost FP F_1, with different direction of the momenta at the energy under consideration, *i.e.* $E = 5080.51\,\mathrm{cm}^{-1}$. These trajectories mimic the evolution of the classical flow in configuration space near the segment of the 1 : 7 PO whose effect in the quantum mechanics of the system we are trying to analyze. To keep the optical analogy as much as possible, we use a "wavefront representation", plotting trajectory points at equally spaced intervals of time. As can be seen in fig. 3(a), trajectories (rays) first leave i, fan-like spreading under the defocusing effect of F_1. During this interval and until trajectories bounce at caustic a, which acts like a mirror, the classical density around the PO decreases. The "fronts" then move upwards,

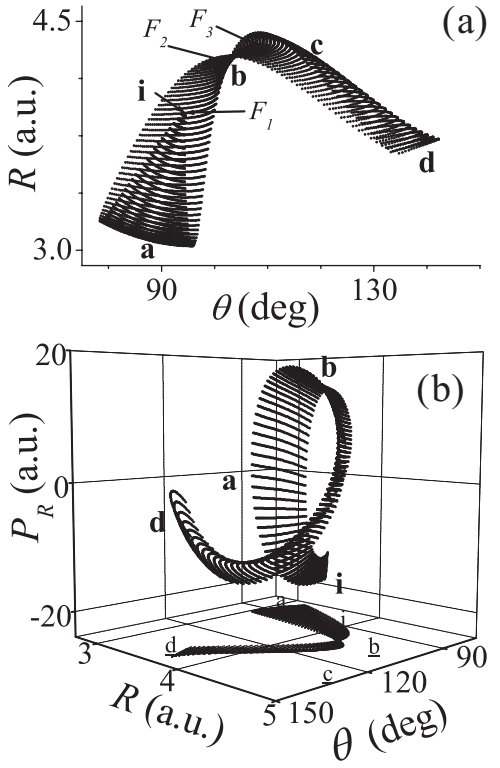

Fig. 3: Illustration of the scarring focusing-defocusing mechanism of trajectories by focal points proposed in the present letter for the case of the bifurcated 1 : 7 periodic orbit of fig. 1(a). See text for details.

keeping (approximately) parallel to each other. So far, this behavior is not very different from that found for an isolated FP —the only acting mechanism in the case of a completely unstable PO— which first focuses and then defocuses the flow of trajectories. However, the situation in the case of a bifurcated PO, like ours, is completely different, since the next FP encountered by the trajectories is not very far away. Indeed, when our diverging trajectory beam "collides" with $F_{2,3}$ (near b and c) it is refocused, so that the amount of classical density in the vicinity of the PO is (approximately) conserved. This action is reinforced by nearby bifurcated POs with similar topologies, in particular the SNB companion and the corresponding family of 1 : 7 Farey tree daughters with higher periods [25]. The result is a self-organized family of FPs forming a quite narrow corridor in configuration space, which like a wave guide prevents the trajectory flow from escaping the PO neighborhood. This can be interpreted as the final result of a focusing-defocusing scarring mechanism existing in this part of the phase space. Notice that this means that chaos channels density in this case, not as usually, by barriers but by a series of traps formed by the FPs. Finally, the bunch of trajectories in fig. 3(a) progress to the right (towards d), as ϑ increases. It is during this phase that a folding of the fronts happens.

Although the above-described dynamics are complex, it is easily be visualized in phase space. The most suitable projection is depicted in fig. 3(b), where the rotating effect of the FPs becomes evident. At i, trajectories form a (mostly) vertical segment which rotates around the propagation direction, as it progresses towards caustic a. There, the front has rotated $\sim 90°$, thus appearing (almost) horizontal. This configuration is maintained until trajectories reach region b, where the folding process starts. At c, the folding is completed, and both configuration and orientation are maintained until region d is reached. In this process the trajectories have completed one turn of an helical motion in phase space. This corresponds to a full period in R while advancing only slightly in the ϑ-direction. Note also that the rotation of the trajectories manifold is highly inhomogeneous, *i.e.* different at each FP. This is due to the strong anharmonicities inherent in the floppy potential describing our system. This methodology provides a way to visualize the whole dynamical process giving rise to scars based on "interactions" between nearby PO FPs acting differently on the trajectory flux.

Numerical argument. – The previous qualitative arguments can be translated into quantitative results with the aid of eqs. (3) and (5). For this purpose, we will analyze separately the two parts entering in each term of the Green function (3).

A striking image of how the classical density accumulates is obtained from the consideration of the caustics of the system. In this case, caustics are formed by the projection into configuration space of the previously described folds. They can be computed from the FP condition, $D = 0$, and their formation illustrated by considering the evolution of an ensemble of neighboring orbits. Results for trajectories starting at the lower $E = 5080.51\,\mathrm{cm}^{-1}$ equipotential (inner R turning points) are shown in fig. 4(a). It is clearly seen that the resulting caustics presents a very complicated shape. For the sake of the discussion, they will be divided into seven different parts, labelled by different letters (colors), a–g, respectively. Trajectories starting at a (red) and g (dark green) give rise, after an elapsed time of $\sim T_R/2$ being T_R the typical oscillation time along coordinate R in this region, to a "normal" linear caustic at the outer turning points (black points in the upper part of the figure). Other trajectories have two or three conjugate points, thus producing anomalous singular caustics with discontinuities. Indeed, orbits in b, c, d, and e (black, light green, blue and orange, respectively) first form, at $\sim T_R/2$, a "swallowtail" [23] in the upper central part of the figure (see blow-up in the inset), and later a smooth curved caustic nearby. We call this inner portion of the caustic part I. Also, orbits starting in b, c and d originate at longer times, ($\sim T_R$), an inner fold caustic (called part II), connecting diagonally the upper and lower equipotentials in the rightmost part of the figure. Finally, trajectories in f give rise to another fold caustic (part III) running vertically in the central part

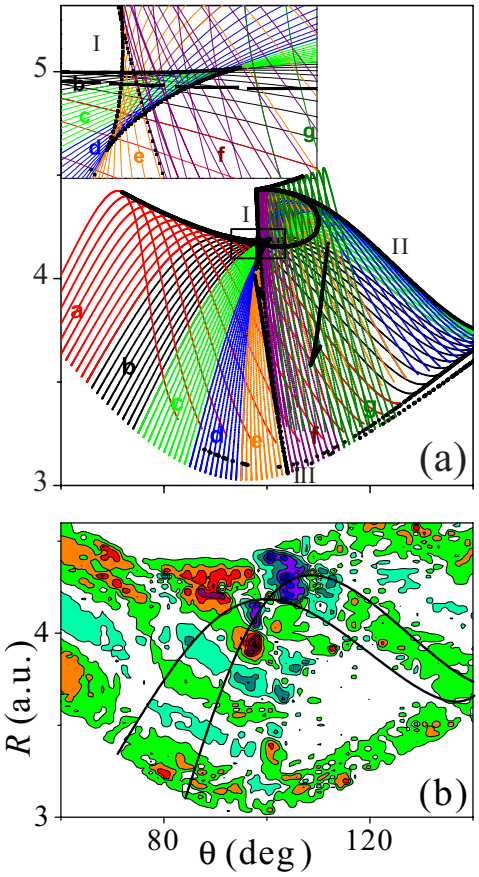

Fig. 4: (Color online) (a) Illustration of caustic formation obtained by propagating trajectories starting in the lower equipotential at the same energy. Letters and colors label trajectories originating different parts of the caustics: I, II, and III (see text for details). The inset zooms in the interesting swallowtail caustic. (b) Imaginary part of the smoothed semiclassical Green function, $G(x,x;E)$, for $E=5080.51\,\mathrm{cm}^{-1}$. An obvious scar by the horseshoe legs of the saddle-node pair of the $1:7$ periodic orbits (superimposed to the figure) is apparent.

of the figure. The influence of these different portions of the caustic, concentrating the classical density, is apparent in the wave functions of fig. 2. Particularly relevant are accumulations on part I for all states, and on part II for states $n=105$, 107 and 112. Notice that it is in the region, filled by trajectories from b–d, that the focusing-defocusing mechanism of FPs $F_{1,2,3}$ acts, channelling the corresponding classical density, as discussed above in connection with the results of fig. 3. The influence of part III of the caustic is apparent in states $n=107$ and 118.

Once the structure of the caustics arising from the pre-exponential part of eq. (3) has been analyzed, let us consider interference, that can be crucial in situations like ours [14]. To examine this effect, we present in fig. 4(b) $\langle \mathrm{Im}\, G(x,x;E)\rangle$, where the averaging is made over an energy window corresponding to the states shown in fig. 2. evaluated using a very dense set of retracing trajectories evenly distributed in the interval $45^\circ \leqslant \vartheta \leqslant 145^\circ$ along the two equipotentials corresponding to $E=5080.51\,\mathrm{cm}^{-1}$. Contributions at every pixel were computed from all trajectories starting and returning to it, by using only the shortest classical paths which included the nearest turning point. The integration time along these PO segments was taken as $\sim 3T_R$. This choice is long enough to guarantee the development of the desired interference effects, while ensuring at the same time that contributions from longer times are not relevant, since they vanish exponentially fast. Similarly, the contribution of longer paths of the same type returning after longer periods is also negligibly small. Remark that the segments of trajectories we used efficiently mimic the POs structure controlling the Green function. For one thing, since POs are dense in the phase space, it is possible to use the associated Farey tree and construct an infinite set of trajectories with dynamically close to the central ($1:7$ in this case) PO, in the sense that that they can be pruned to approach as much as wanted to it. Actually, the shape of these orbits do not differ significantly from the central PO near the ends, although they may be very different, both in length and period, elsewhere. Second, all unstable trajectories starting at these ends will eventually finish their evolution also at ends, thus producing self-reverse orbits. Figure 4(b) demonstrates that our surrogate of the (true) semiclassical wave function shows clear evidence of scarring along the horseshoe leg of the bifurcated $1:7$ PO and its companion, both being shown also in the figure. For example, the number of nodes along this segment is five, in perfect agreement with the partial scars visible in most wave functions presented in fig. 2. Moreover, the accumulation of density along the corresponding caustics is also apparent, being then a robust effect which is not destroyed by the interference with other families of POs.

Summary and conclusions. – Since first discussed by Heller, scarring has occupied a prominent position in the studies of the correspondence between quantum and classical dynamics in chaotic systems. The reason is twofold. First, scars constitute a privileged and straightforward indicator showing how classical invariants appear in the quantum theory. Second, the consequences of such a peculiar dynamics are also important at practical and technological level. Although there still remain non-trivial open questions, we have at present a fairly good understanding of the scarring of isolated POs, developed over the seminal ideas of Heller [3] and Bogomolny [6].

However, much less is known about scarring in systems with mixed dynamics, despite the fact that they represent the generality in many fields of physics, and also that it is known that scars show here spectacular differences [14]. In this letter, we have discussed a new mechanism of scarring in this type of systems, presenting supporting numerical evidence obtained in a realistic model for the LiCN molecule. Here, the accumulation of probability takes place through a combined focusing-defocusing effect of the FPs of the scarring PO, this "dressing" some parts

of the corresponding trajectories. The effect is reinforced by longer POs arising in the related infinite chain of bifurcations. This opens an interesting line of research that will be undoubtedly fruitful. For example, questions such as, what happens to this mechanism in the true semiclassical limit, or predicting the energy intervals in which this mechanism prevails are points that should be addressed in the near future. We also remark that, although the work presented here has been carried out at an energy far above the bifurcation point, our mechanism should bear some sort of connection or complementarity with the superlocatization of probability density discussed by Keating and Prado [14]. In our opinion this is a point worth considering in the future.

Finally, let us briefly comment on the physical implications of this scarring effect in the dynamics of the LiNC/LiCN isomerization reaction. The phenomenon discussed here implies highly excited motion in the R coordinate, that, by connecting the two equipotentials branches, form dividing surfaces [16,19], which act similarly to a continental divide separating different watersheds, for the reactive motion along ϑ. Such dynamical barriers in phase space produce classical bottlenecks [26]. Here we have unveiled —for a realistic chemical example— the profound effect that these objects have at the quantum level; *i.e.*, the barriers manifest as a strong localization of the wave functions. The consequences in the isomerization reaction are currently being investigated by considering the associated flux matrix elements.

* * *

Support from MICINN-Spain under contracts No. MTM2009-14621 and iMath-CONSOLIDER 2006-32) is fully acknowledged.

REFERENCES

[1] Kaplan L. and Heller E. J., *Ann. Phys. (N.Y.)*, **264** (1998) 171.
[2] Kaplan L., *Nonlinearity*, **12** (1999) R1.
[3] Heller E. J., *Phys. Rev. Lett.*, **53** (1984) 1515.
[4] Gutzwiller M. C., *Chaos in Classical and Quantum Mechanics* (Springer Verlag, New York) 1990.
[5] Heller E. J., in *Chaos and Quantum Physics*, edited by Giannoni M. J., Voros A. and Zinn-Justin J. (Elsevier, Amsterdam) 1991.
[6] Bogomolny E. B., *Physica D*, **31** (1988) 169.
[7] de Polavieja G. G., Borondo F. and Benito R. M., *Phys. Rev. Lett.*, **73** (1994) 1613.
[8] Wisniacki D. A., Vergini E., Benito R. M. and Borondo F., *Phys. Rev. E*, **70** (2004) 035202(R); *Phys. Rev. Lett.*, **94** (2005) 054101; **97** (2006) 094101.
[9] Berry M. V., *Proc. R. Soc. London, Ser. A*, **243** (1989) 219.
[10] Sridhar S., *Phys. Rev. Lett.*, **67** (1991) 785; Dörr U., Stöckman H.-J., Barth M. and Kuhl U., *Phys. Rev. Lett.*, **80** (1998) 1030.
[11] Wilkinson P. B., Fromhold T. M., Eaves L., Sheard F. W., Miura N. and Takamasu T., *Nature (London)*, **380** (1996) 608; Fromhold T. M., Wilkinson P. B., Sheard F. W., Eaves L., Miao J. and Edwards G., *Phys. Rev. Lett.*, **75** (1995) 1142; Crook R., Smith C. G., Graham A. C., Farrer I., Beere H. E. and Ritchie D. A., *Phys. Rev. Lett.*, **91** (2003) 246803.
[12] Doya V., Legrand O., Mortessagne F. and Miniatura C., *Phys. Rev. Lett.*, **88** (2001) 014102; Michel C., Doya V., Legrand O. and Mortessagne F., *Phys. Rev. Lett.*, **99** (2007) 224101.
[13] Huang L., Lai Y.-C., Ferry D. K., Goodnick S. M. and Akis R., *Phys. Rev. Lett.*, **103** (2009) 054101.
[14] Keating J. P. and Prado S. D., *Proc. R. Soc. London, Ser. A*, **457** (2001) 1855.
[15] Berry M. V., Keating J. P. and Prado S. D., *J. Phys. A*, **31** (1998) L245; Berry M. V., *Phys. Scr.*, **T90** (2001) 15; Bäcker A., Keating J. P. and Prado S. D., *Nonlinearity*, **15** (2002) 1417.
[16] Borondo F. and Benito R. M., in *Non-Linear Dynamics and Fundamental Interactions*, edited by Khanna F. and Matrasulov D., *NATO Sci. Ser. II*, Vol. **213** (Springer, Dordrecht) 2006.
[17] Borondo F., Vergini E., Wisniacki D. A., Zembekov A. A. and Benito R. M., *J. Chem. Phys.*, **122** (2005) 111101.
[18] Prado S. D., Vergini E., Benito R. M. and Borondo F., *EPL*, **88** (2009) 40003.
[19] Zembekov A. A., Borondo F. and Benito R. M., *Chem. Phys. Lett.*, **246** (1995) 421; Borondo F., Zembekov A. A. and Benito R. M., *J. Chem. Phys.*, **105** (1996) 5068.
[20] Benito R. M., Borondo F., Kim J. H., Sumpter B. G. and Ezra G. S., *Chem. Phys. Lett.*, **161** (1989) 60.
[21] Bacic Z. and Light J. C., *J. Chem. Phys.*, **85** (1986) 4595.
[22] Gutzwiller M. C., *J. Math. Phys.*, **12** (1971) 343.
[23] Poston T. and Stewart I., *Catastrophe Theory and its Applications* (Pitman, Boston) 1978.
[24] Zembekov A. A., *Chem. Phys. Rep.*, **19** (2001) 1783.
[25] Buchleitner A., d'Arcy M. B., Fishman S., Gardiner S. A., Guarneri I., Ma Z.-Y., Rebuzzini L. and Summy G. S., *Phys. Rev. Lett.*, **96** (2006) 164101.
[26] Jaffé C., Farrelly D. and Uzer T., *Phys. Rev. Lett.*, **84** (2000) 610; Bartsch T., Hernandez R. and Uzer T., *Phys. Rev. Lett.*, **95** (2005) 058301.